Photoinhibition and recovery of primary photosynthesis in Antarctic and subantarctic lichens. Analysis of interspecific differences

Syed Inzimam Ul Haq[1*], Marta Bravo Benita[2], Sonia de Caralt[2]

[1]*Laboratory of Photosynthetic Processes, Department of Experimental Biology, Faculty of Science, Masaryk University, Kamenice 5, 625 00 Brno, Czech Republic*
[2]*University of Girona, Faculty of Science, Campus Montilivi, 17003, Girona, Spain*

Abstract

This study meticulously investigates the dynamics of photoinhibition and the mechanisms of primary photosynthetic activity recovery in lichens found in Antarctica and the sub-Antarctic regions. Advanced methodologies were utilised, such as Kautsky's kinetic analysis and the OJIP test. The study carefully details the response of various lichen species to intense light stress, outlining both immediate effects and subsequent recovery processes. Our findings reveal that these lichens employ a range of adaptive strategies, specific to each species, to mitigate the effects of photoinhibition, thereby emphasizing their remarkable resilience and ecological importance in harsh environments. Notably, the investigation reveals the sophisticated interplay between inherent photoprotective mechanisms and the ecological adaptations that enable these lichens to thrive under such harsh conditions. The study not only advances our knowledge of plant physiology under stress but also enriches our insights into the survival strategies of terrestrial organisms facing global environmental changes. Three types of photoinhibitory treatments differing in their duration and strength were applied to 7 lichen species from Antarctica and South America (Isla Navarino). The lichens responded with a decrease in photosynthetic processes in photosystem II (F_V/F_M and Φ_{PSII} declined), although they showed almost complete recovery in the following 5 h. This was attributed to the activation of photoprotective mechanisms, non-photochemical quenching (NPQ) in particular, during photoinhibitory treatments. Chlorophyll fluorescence parameters derived from slow Kautsky kinetics were correlated with those derived from the OJIP curve. Our study presents data that supports the conclusion of significant photoresistance of the studied lichen species in the hydrated state to photoinhibition induced by high doses of photosynthetically active radiation (PAR).

Key words: Kautsky's kinetic, lichens, OJIP methods, photoinhibition, photosystem II

DOI: 10.5817/CPR2024-1-4

Received May 24, 2024, *accepted* September 7, 2024.
[*]Corresponding author: Syed Inzimam Ul Haq <syedinzimam74@gmail.com>
Acknowledgements: We would like to express our sincere gratitude to the Laboratory of Photosynthetic Processes at Masaryk University for providing the facilities and resources necessary to conduct this research. Our deepest appreciation goes to Professor Dr. Miloš Barták, for his invaluable guidance, mentorship, and support throughout the duration of this study. Special thanks to our co-author, Dr. Sonia de Caralt from the University of Girona, for her collaboration and insightful contributions.

Introduction

Lichens are remarkably robust organisms with unique characteristics of stress tolerance that allow them to exist in some of the harshest environments on Earth (Armstrong 2017). They are common in the Antarctic and Subantarctic regions, as they experience extreme cold, rampant humidity fluctuations, high wind exposure, and intense UV radiation, among other stressors (Perera-Castro et al. 2021, Colesie et al. 2023). These conditions present a challenge for photosynthetic organisms. Lichens develop from a symbiotic relationship between fungi and their photosynthetic companions, which can be algae or cyanobacteria (Carr et al. 2021). These species exhibit remarkable adaptations that allow them to survive for long periods and flourish naturally under extreme conditions. Therefore, lichens are ecologically important and can live long enough to contribute a higher percentage of terrestrial biomass in some of the exposed spaces (Armstrong 2021). Lichen habitats are microhabitats with high levels of light exposure. Photoinhibition is the reduction in photosynthesis under the influence of solar radiation (Pospíšil 2016). It occurs when photosynthetic organisms absorb more light than they can use, damaging the photosynthetic apparatus. This is ultimately manifested in depressed growth of plants (Zavafer and Mancilla 2021, Shi et al. 2022). Photoinhibition of photosynthesis is characterized by partial photodestruction of PSII, partial involvement of photoprotective reactions, and resynthesis processes with gradual restoration of PSII (Balarinova et al. 2014). Barták et al. (2021) conducted a recent study on how thallus desiccation affects primary photosynthetic processes. According to the findings of this study, in lichen photobionts, when their relative water content (RWC) decreases to less than 20%, defense mechanisms on the chloroplastic apparatus are initiated (Barták et al. 2021). Similarly, in 2023, Barták et al. investigated the alternations in primary photochemical processes of photosystem II due to a temporary photoinhibitory impact and concluded that *Xanthoria elegans* has effective non-photochemical quenching mechanisms in addition to a high degree of resistance against photoinhibition (Barták et al. 2023). Lichens in regions with high solar radiations, such as Antarctica, face physiological challenges due to photoinhibition. A detailed comprehension of the intricate mechanisms underlying photoinhibition and the subsequent recovery processes is necessary to comprehend how lichens adjust to and regulate high levels of sun radiation. The responses of photosynthetic mechanisms to light stress and their recovery were examined in this study using advanced techniques, such as Kautsky's kinetic method and the OJIP test. The chlorophyll fluorescence of plants is altered by the Kautsky effect, which occurs as plants move from darkness to light. This impact offers important information regarding the photosynthetic activity and general health of plants under stressful circumstances (Aucique-Perez and Ramos 2024). Chlorophyll fluorescence is a noninvasive method that provides information on a plant's photosynthetic system. It is an indicator of the stress effects on plants (Kohzuma et al. 2021). One of the key methods to measure the efficiency of photosynthesis is through the use of the OJIP test. This was achieved by examining the sharp rise in fluorescence triggered by chlorophyll, also referred to as the induction curve (Khan et al. 2021, Akinyemi et al. 2023). The OJIP test helps us analyze the issues that occur before and after photoinhibition with photosystem II (PSII) efficiency. OJIP includes O, J, I, and P points, through which the electron transport processes in PSII can be analyzed (Zabret and Nowaczyk 2021). These approaches are crucial for understanding the complex photosynthetic re-

sponses of lichens that include *Pseudocyphellaria glabra*, *Nephroma antarcticum*, *Cladonia* sp., *Himantormia lugubris*, *Ramalina terebrata*, *Parmelia* sp. and *Physcia* sp. We chose these lichens based on their distribution within the diverse microclimates of the Antarctic and sub-Antarctic regions. Antarctic lichens exhibit varying levels of photoinhibitory resistance. Researchers have found that certain lichens, such as *Xanthoria elegans* (Barták et al. 2023) and moss *Sanionia uncinata* (Orekhova et al. 2021), as well as various macrolichens (Barták et al. 2021), effectively protect themselves from high levels of light stress. These lichens experience minimal photoinhibition, meaning that they can quickly recover after exposure to intense light. The Antarctic lichens *Usnea antarctica* and *U. aurantiaco-atra* have been studied under medium light stress conditions. The results revealed differences in their susceptibility to photoinhibition, with *U. antarctica* displaying a higher resistance. Further analysis of chlorophyll fluorescence parameters and pigment content variations support the resilience of Antarctic lichens to photoinhibitory conditions (Balarinova et al. 2014). Antarctic lichens have developed strong strategies to protect themselves from excessive sunlight, allowing them to thrive even in challenging, high-light environments. Lichens, such as *Cetraria islandica*, *Lobaria pulmonaria*, *Peltigera aphthosa*, *P. membranacea*, *Pseudocyphellaria gilva*, and *Sticta sublimbata* showed resistance to photoinhibition (Ndhlovu et al. 2023). These lichens exhibit different levels of sensitivity to sunlight. Pale colored lichens are more likely to experience photoinhibition, compared to dark colored lichens (Mafole et al. 2017). Moreover, desiccation inhibits photosynthesis in lichens, making them susceptible to photoinhibition, which highlights lichens' reliance on desiccation-induced chlorophyll quenching for photoprotection (Wieners et al. 2018). In addition, *Xanthoria elegans*, a lichen from Antarctica, demonstrates remarkable resistance to photoinhibition through effective photoprotective mechanisms, enabling it to tolerate short-term exposure to high-light levels (Barták et al. 2023). In these studies, diverse responses of lichens to photoinhibition, as well as protective mechanisms, contributed to their survival in high-light environments. Therefore, we hypothesized that these seven lichen species collected from Antarctica and the sub-Antarctic regions would show different reactions to photoinhibition and recovery. This will be influenced by their unique ecological adaptations and physiological traits. Specifically, we expect that lichens from different microhabitats (with varying light exposure and moisture levels) will show varying degrees of photoinhibition and recovery, reflecting their local environmental adaptations. The selected species represent a diverse array of ecological niches and physiological characteristics, offering a comprehensive understanding of the factors impacting their ability to withstand extreme light conditions. Furthermore, a strong and positive relationship is expected between the maximal quantum yield (F_V/F_M) of PSII and the performance index on an absorption basis (PI_{ABS}): lichens with higher photochemical yield are expected to be less stressed and will cope significantly better.

Material and Methods

Lichen collection and management

Lichen species, such as *Pseudocyphellaria glabra*, *Nephroma antarcticum*, *Cladonia* sp., *Himantormia lugubris*, *Ramalina terebrata*, *Parmelia* sp. and *Physcia* sp. (*see* Fig. 1), were collected from the Antarctic and subantarctic regions during the winter field camps (January to March 2024). Lichens were collected at Navarino Island (54.9604 S, 67.6557 W, 210 m a.s.l.), King George Island (62.1792 S, 58.9104 W, 35 m a.s.l.), and Galindez Island (65.2458 S, 64.2578 W, 18 m a.s.l.) (*see* Table 1). The samples were shipped to a lab in Brno, Czech Republic in a dry state. The thalli were re-wetted 48 or 72 hours before the start of experiments. The thalli were regularly soaked with demineralized water after being placed into Petri dishes with Pur-Zellin® Hartmann wadding. Fluorometric testing was used to confirm optimal hydration. Upon reaching its maximum levels, F_V/F_M indicated that the sample was optimally hydrated. The thalli were kept at 5°C and exposed to low irradiance of 10 µmol m^{-2} s^{-1} PAR. Sampling sites were selected to encompass a different range of ecological conditions, including variations in substrate type, moisture levels, and light exposure.

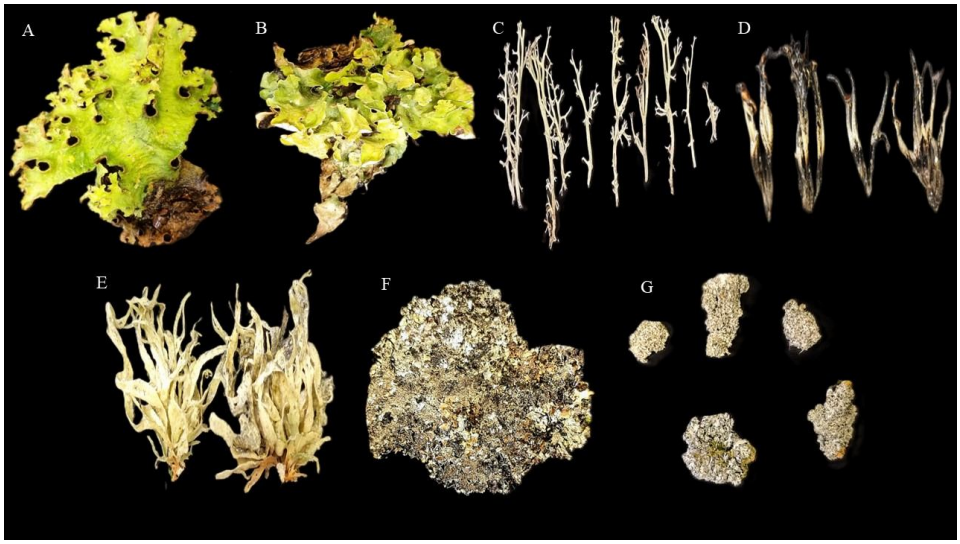

Fig. 1. Lichen species used for photoinhibition experiments: (A) *Pseudocyphellaria glabra*, (B) *Nephroma antarcticum*, (C) *Cladonia* sp., (D) *Himantormia lugubris*, (E) *Ramalina terebrata*, (F) *Parmelia* sp. and (G) *Physcia* sp.

Light stress exposure

Lichen thalli were exposed to three different light intensities such as 1 000 µmol m^{-2} s^{-1} (1 hour), 2 000 µmol m^{-2} s^{-1} (1 hour), and 2 000 µmol m^{-2} s^{-1} (2 hours) to induce short-term photostress. A homogeneous light source was used, consisting of a special LED setup (UTEE, Technical University Brno, Czech Republic) with 17 high-

intensity warm white LEDs (Luxeon Warm -White, Philips Lumileds, USA), emitting a continuous light spectrum. Thalli from various species such as *Parmelia* sp., *Nephroma antarcticum*, *Ramalina terebrata*, *Himantormia lugubris*, *Cladonia* sp., *Parmelia* sp., and *Physcia* sp. were placed horizontally in separate petri dishes for exposure. During the exposure, the thalli were kept moist. During the recovery phase, the thalli were covered with cellulose paper moistened with demineralized water (Pur-Zellin®, HartMann) at regular intervals to prevent desiccation stress.

Chlorophyll fluorescence measurements

The impact of high-intensity light on experimental lichen species, and the PSII of their photobionts, respectively, were assessed using several chlorophyll fluorescence measurements. The values of the chlorophyll fluorescence parameters were recorded in the experiment: (a) before photoinhibitory treatment (Control), (b) after photoinhibition, followed by recovery phases (c) 30 min., (d) 60 min., (e) 120 min. and finally (f) 180 min. after the photoinhibitory treatment. The recovery period was carried out in laboratory conditions (under 10 $\mu mol\ m^{-2}\ s^{-1}$). A FluorCam (HFC-010, Photon Systems Instruments, Czech Republic) fluorometer was used for the measurements of chlorophyll fluorescence. To evaluate the effect of photoinhibitory treatment, slow Kautsky kinetics (KK) supplemented with quenching analysis were used (for method *see* e.g. Barták et al. 2023). The chlorophyll fluorescence parameters assessed included F_V/F_M, Φ_{PSII}, F_o/F_t, relative fluorescence decrease (RFD), and non-photochemical quenching (NPQ).

Fast chlorophyll fluorescence transients (OJIPs) measurements

Fast chlorophyll fluorescence transients (OJIPs) were recorded using a FluorPen FL 1000 fluorometer (Photon Systems Instruments, Czech Republic) to evaluate the effects of photoinhibitory treatment on photosystem II (PSII) functionality. Measurements were taken at several time points: before the photoinhibitory treatment as a control, immediately after exposure to 2 000 $\mu mol\ m^{-2}\ s^{-1}$ for 120 min., and during recovery at 60 and 180 min. post-treatment following a 5-min. dark adaptation period. The FluorPen software (Photon Systems Instruments, Drásov, Czech Republic) was used to extract parameters from OJIP curves. These parameters offer insights into the yields and energy fluxes absorbed per PSII reaction center and/or per cross section. Some of the parameters selected for detailed analysis included the photosynthetic performance index (PI_{ABS}), the initial donor side limitation per PSII reaction center (DI_o/RC), and the electron transport rate per reaction center (ET_o/RC).

Statistical Analysis

The data were statistically analyzed by analysis of variance (ANOVA) using SPSS 20 software. The mean ± standard deviation (SD) of five separate replications was reported. GraphPad Prism 9.0.0 was used for plotting figures.

Species	Collection site	Site characterization
Pseudocyphellaria glabra	Navarino Is.	Tierra del Fuego. Notophagus-dominated forest floor. Annual mean air temperature 6.0°C.
Nephroma antarcticum	Navarino Is.	Tierra del Fuego. Notophagus-dominated forest floor. Annual mean air temperature 6.0°C.
Cladonia sp.	Navarino Is.	Tierra del Fuego. Forest-free tundra. Wet place. Annual mean air temperature 6.0°C.
Himantormia lugubris	King George Is.	Fildes peninsula, neighbourhood of Artigas station, Antarctica. Annual mean air temperature -0.9°C.
Ramalina terebrata	King George Is.	Fildes peninsula, neighbourhood of Artigas station, Antarctica. Annual mean air temperature -0.9°C.
Parmelia sp.	Galindez Is.	Coastal vegetation oasis. Mean annual air temperature -4.0°C.
Physcia sp.	Galindez Is.	Coastal vegetation oasis. Mean annual air temperature -4.0°C.

Table 1. Collection sites and site characterization of various lichen species.

Results

Photoinhibition-induced decrease in F_V/F_M and consequent recovery

Figure 2 illustrates the photoinhibition and subsequent recovery effects on the maximum quantum yield of PS II (F_V/F_M) in Antarctic and sub-Antarctic lichens exposed to 1 000 µmol m^{-2} s^{-1} for one hour and 2 000 µmol m^{-2} s^{-1} for one and two hours. Significant decreases in F_V/F_M were observed due to photoinhibition across all species, followed by a recovery. ANOVA indicated significant differences among species ($p < 0.0001$). *P. glabra* showed a 46.3% decrease in F_V/F_M after exposure to 1 000 µmol m^{-2} s^{-1} for one hour, recovering to 97.1%, but did not return to control levels. Severe photodamage was observed after exposure to 2 000 µmol m^{-2} s^{-1} for one hour (78.3% decrease) and two hours (77.5% decrease), with incomplete recovery (89.1% and 91.3%, respectively). *N. antarcticum* experienced a 46.3% decrease after exposure to 1 000 µmol m^{-2} s^{-1} for one hour, recovering to 94.2%. Severe photodamage occurred after exposure to 2 000 µmol m^{-2} s^{-1} for one hour (58.4% decrease) and two hours (58.4% decrease), with partial recovery (86.3% and 90.7%, respectively). *R. terebrata* exhibited the highest susceptibility with a 95.1% decrease after exposure to 1000 µmol m^{-2} s^{-1} for one hour, recovering to 85.4%. A 57.4% decrease was observed after exposure to 2 000 µmol m^{-2} s^{-1} for one hour, recovering to 79.6%. *H. lugubris* showed an 80.2% decrease after exposure to 1 000 µmol m^{-2} s^{-1} for one hour, with almost complete recovery (93.8%). A 29.6% decrease after exposure to 2000 µmol m^{-2} s^{-1} for one hour, recovering to 96.2%. The data reveals that exposure to 2 000 µmol m^{-2} s^{-1} light intensity for one hour causes significant photodamage with an F_V/F_M ratio of 47.6%, rising to 100% during final recovery. *Cladonia* sp. experienced a 59.3% decrease after exposure to 1 000 µmol m^{-2} s^{-1} for one hour, with a final recovery of 93.2%. A notable early decline (29.6%) after 2 000 µmol m^{-2} s^{-1} for one hour, with a final recovery of 96.2%. *Parmelia* sp. exhibited an 85.7% decrease after exposure to 1 000 µmol m^{-2} s^{-1} for one hour, with complete recovery. Severe photodamage (44.7% decrease) after exposure to 2000 µmol m^{-2} s^{-1} for one hour, recovering to 97.3%.

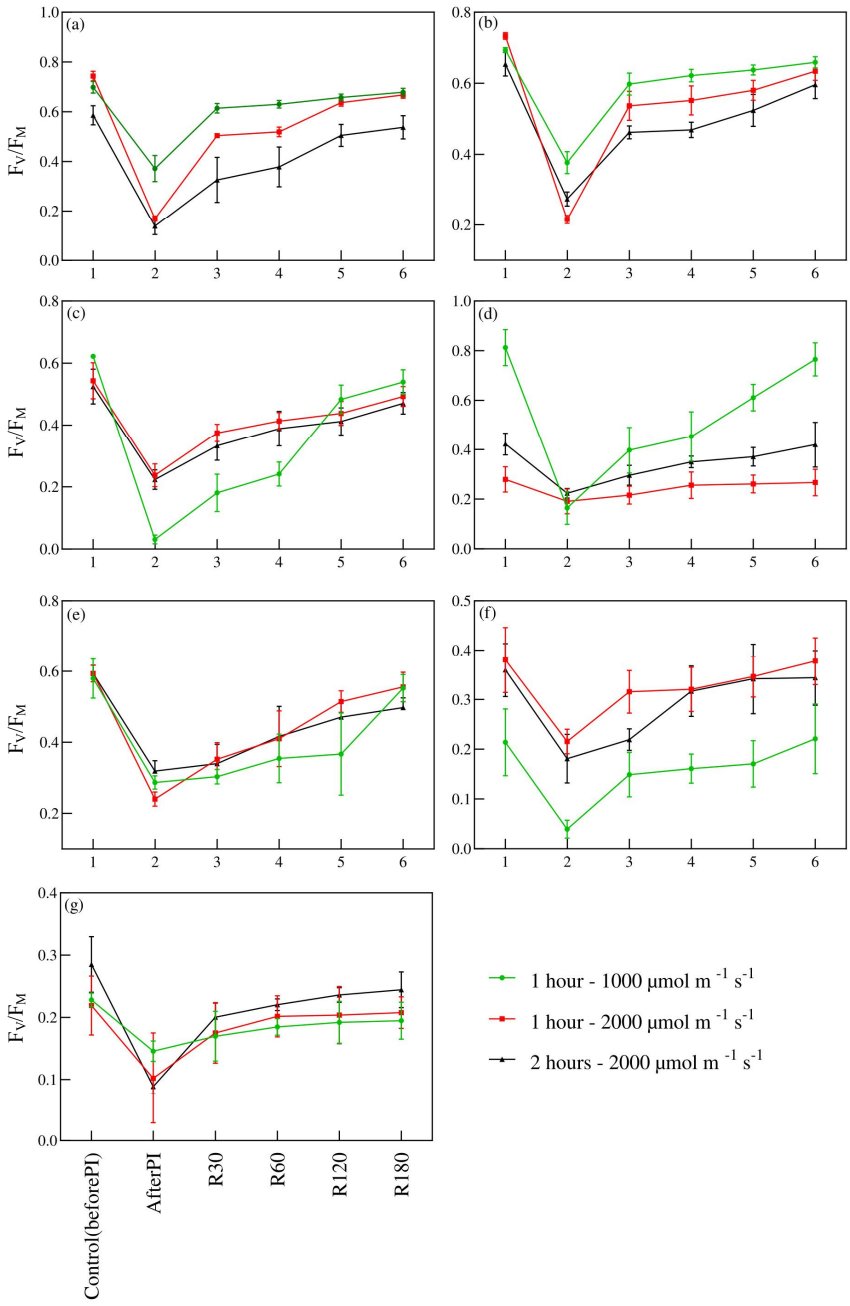

Fig. 2. Time courses of the maximum quantum yield of photosystem II (F_V/F_M), recorded in (a) *Pseudocyphellaria glabra*, (b) *Nephroma antarcticum*, (c) *Ramalina terebrata*, (d) *Himantormia lugubris*, (e) *Cladonia* sp., (f) *Parmelia* sp. and (g) *Physcia* control (before PI), immediately after the photoinhibitory treatment (after PI), and after 30, 60, 120, and 180 min. recovery (R30, R60, R120, and R180). Data points represent the means of five replicates ± standard deviations (error bars).

Furthermore, after exposure to 2 000 µmol m^{-2} s^{-1} for two hours, the F_V/F_M ratio showed a slow improvement, implying some recovery of photosynthetic efficiency up to 97.1%. *Physcia* showed a 36.3% decrease after exposure to 1 000 µmol m^{-2} s^{-1} for one hour, recovering to 86.3%. Severe photodamage (52.3% decrease) was observed after exposure to 2 000 µmol m^{-2} s^{-1} for one hour, recovering to 95.2%. Post-hoc Tukey's analysis indicated significant recovery differences between species, with *Parmelia* sp. and *N. antarcticum* exhibiting strong recovery rates, while *R. terebrata* and *H. lugubris* showed greater susceptibility to photodamage.

Photoinhibition-induced decrease in Φ_{PSII} and consequent recovery

Figure 3 illustrates the recovery of the quantum yield of PS II (Φ_{PSII}) in different lichen species following photoinhibition. ANOVA results confirm significant differences across conditions for all species ($p < 0.001$). *P. glabra* exhibited full recovery of Φ_{PSII} to 100% after a 19.8% inhibition when exposed to 1 000 µmol m^{-2} s^{-1} for one hour. However, after exposure to 2 000 µmol m^{-2} s^{-1} for one hour, Φ_{PSII} decreased by 55.7% but recovered to 94.7%, and after two hours of exposure, Φ_{PSII} declined by 71%, recovering to 86.8%, indicating some resilience (Fig. 3a). In *N. antarcticum*, Φ_{PSII} decreased by 58.2% after exposure to 1 000 µmol m^{-2} s^{-1} for one hour, recovering to 100%. However, at exposure of 2 000 µmol m^{-2} s^{-1} for one hour, Φ_{PSII} efficiency decreased by 58.2%, gradually increasing to 76.7% during recovery, and after two hours of exposure, Φ_{PSII} decreased by 76.6%, recovering to 83.3% during the final recovery phase (Fig. 3b). *R. terebrata* showed a 95.1% decrease in Φ_{PSII} after exposure to 1 000 µmol m^{-2} s^{-1} for one hour, recovering to 81.9%, and completely recovered to 100% after inhibition by 38.5% at exposure of 2 000 µmol m^{-2} s^{-1} for one hour. After two hours of exposure to 2 000 µmol m^{-2} s^{-1}, Φ_{PSII} recovered to 96.8% after inhibition up to 41.6%, indicating restored photosynthetic function (Fig. 3c). *H. lugubris* displayed a consistent increase up to 81.4% in Φ_{PSII} during recovery after 66.6% photoinhibition at 1 000 µmol m^{-2} s^{-1} for one hour. Complete recovery of Φ_{PSII} was observed after exposure to 2 000 µmol m^{-2} s^{-1} for one hour, and after two hours of exposure, Φ_{PSII} increased to 97.7% during recovery (Fig. 3d). *Cladonia* sp. showed a consistent 90.4% increase in Φ_{PSII} during recovery after 35.6% inhibition by 1 000 µmol m^{-2} s^{-1} exposure for one hour. Φ_{PSII} gradually recovered after 59.3% inhibition by 2 000 µmol m^{-2} s^{-1} exposure for one hour, reaching 100%, and after two hours of exposure, Φ_{PSII} increased to 83.3% during recovery (Fig. 3e). *Parmelia* sp. showed an 88.7% inhibition after 1 000 µmol m^{-2} s^{-1} exposure for one hour, with a progressive increase up to 92.8% in Φ_{PSII} during recovery. After exposure to 2 000 µmol m^{-2} s^{-1} for one hour, Φ_{PSII} declined by 39.4%, then recovered to 89.6%, and after two hours exposure, Φ_{PSII} indicated a recovery of up to 92.8% (Fig. 3f). In *Physcia*, an initial decline in Φ_{PSII} up to 38.3% was observed after exposure to 1 000 µmol m^{-2} s^{-1} for one hour followed by a recovery to 90.9%. After exposure to 2 000 µmol m^{-2} s^{-1} for one hour, Φ_{PSII} decreased by 69.6%, recovering to 94.7%, and a sustained increase in Φ_{PSII} was observed, reaching up to 95% during recovery following 67.3% inhibition caused by 2 000 µmol m^{-2} s^{-1} exposure for two hours (Fig. 3g). Post-hoc Tukey's analysis indicated significant recovery differences between species, with *P. glabra* and *N. antarcticum* showing the highest resilience, while *R. terebrata* and *H. lugubris* displayed slower recovery rates.

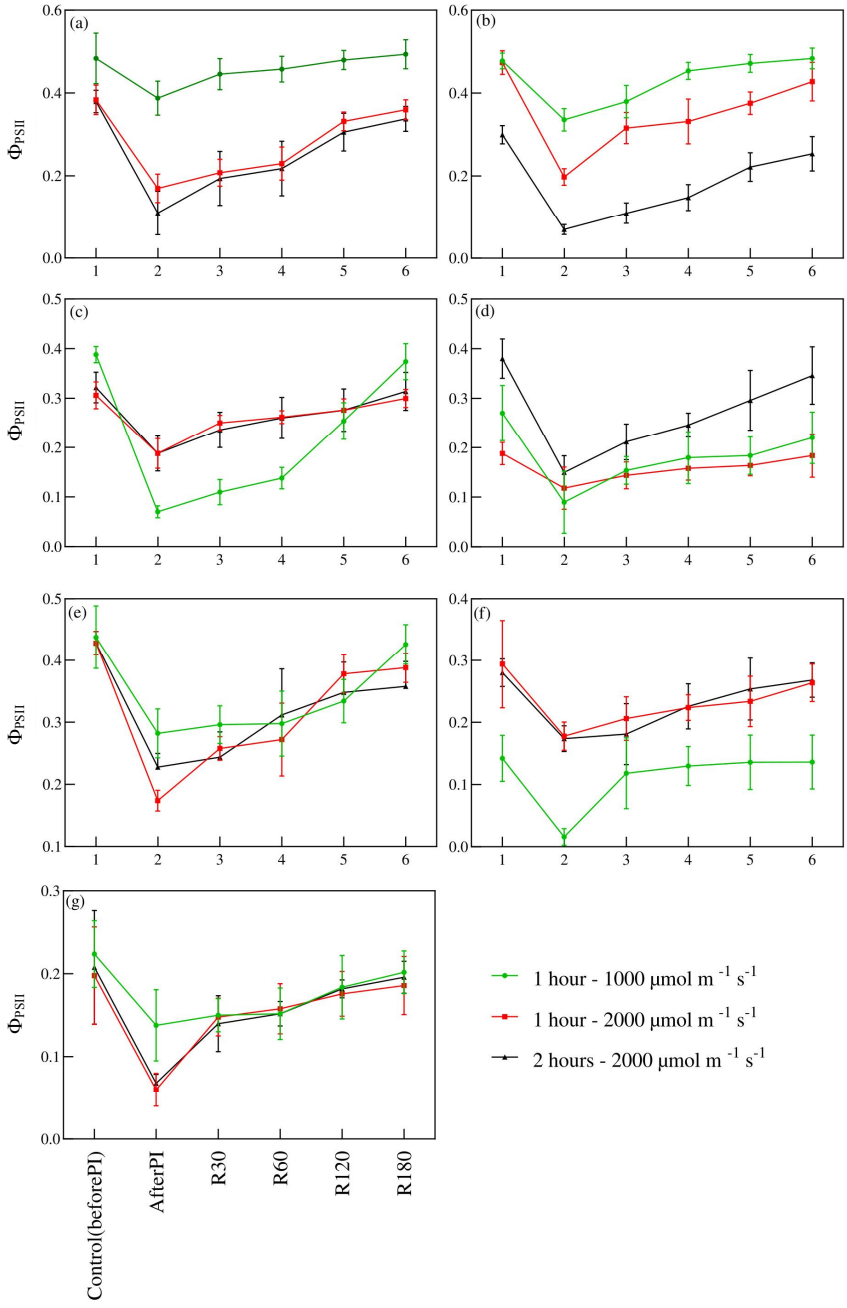

Fig. 3. Time courses of the quantum yield of photosystem II (Φ_{PSII}), recorded in (a) *Pseudocyphellaria glabra*, (b) *Nephroma antarcticum*, (c) *Ramalina terebrata*, (d) *Himantormia lugubris*, (e) *Cladonia* sp., (f) *Parmelia* sp., and (g) *Physcia* control (before PI), immediately after the photoinhibitory treatment (after PI), and after 30, 60, 120, and 180 min. recovery (R30, R60, R120, and R180). Data points represent the means of five replicates ± standard deviations (error bars).

Photoinhibition-induced decrease in F_o/F_t and consequent recovery

Figure 4 illustrates the recovery trends of the F_o/F_t ratio in different lichen species following photoinhibition. ANOVA results indicated significant differences among species, light levels, and exposure times ($p < 0.01$). *P. glabra* showed an increasing trend in F_o/F_t during recovery up to 96.3% after photoinhibition (decrease from control) of 29% at an exposure of 1 000 µmol m^{-2} s^{-1} for one hour but did not completely return to control values, indicating susceptibility to prolonged exposure to intense light. After photoinhibition of 54% at an exposure of 2 000 µmol m^{-2} s^{-1} for one hour, recovery was incomplete, reaching only 90.5%. Further, after photoinhibition of 72.7% at an exposure of 2 000 µmol m^{-2} s^{-1} for two hours, F_o/F_t recovered up to 94.3%, staying lower than control levels due to the continuing effect of intense light exposure (Fig. 4a). In *N. antarcticum*, the F_o/F_t ratio declined by 13.41% after exposure to 1 000 µmol m^{-2} s^{-1} for one hour, followed by a complete recovery to 98.7%. After photoinhibition of 49.2% at an exposure of 2 000 µmol m^{-2} s^{-1} for one hour, the Fo/Ft ratio increased to 90.6%, and after photoinhibition of 22.1% at an exposure of 2 000 µmol m^{-2} s^{-1} for two hours, it increased to 99.2% (Fig. 4b). In *R. terebrata*, the F_o/F_t ratio was inhibited by 23.1% after exposure to 1 000 µmol m^{-2} s^{-1} for one hour, followed by recovery to 93.4%, remaining below control ranges. After photoinhibition of 23.2% at an exposure of 2 000 µmol m^{-2} s^{-1} for one hour, the F_o/F_t ratio increased to 97.7%, and after photoinhibition of 51.8% at an exposure of 2 000 µmol m^{-2} s^{-1} for two hours, it rose to 87.8% (Fig. 4c). In *H. lugubris*, the F_o/F_t ratio declined by 7.1% after exposure to 1 000 µmol m^{-2} s^{-1} for one hour, recovering to 99.1%. After photoinhibition of 46.7% at an exposure of 2 000 µmol m^{-2} s^{-1} for one hour, the F_o/F_t ratio recovered to 94.8%, and after photoinhibition of 46.7% at an exposure of 2 000 µmol m^{-2} s^{-1} for two hours, it recovered to 97.6%, though it remained below initial conditions (Fig. 4d). In *Cladonia* sp., the F_o/F_t ratio showed an early decline of 44.6% after exposure to 1 000 µmol m^{-2} s^{-1} for one hour, followed by recovery up to 96.2%. After photoinhibition of 39.2% at an exposure of 2 000 µmol m^{-2} s^{-1} for one hour, the ratio increased to 94.8%, and after photoinhibition of 40.2% at an exposure of 2 000 µmol m^{-2} s^{-1} for two hours, it recovered up to 82.6% (Fig. 4e). In *Parmelia* sp. the F_o/F_t ratio rose to 80.6% after photoinhibition of 52.4% at an exposure of 1 000 µmol m^{-2} s^{-1} for one hour. After photoinhibition of 25.6% at an exposure of 2 000 µmol m^{-2} s^{-1} for one hour, the F_o/F_t ratio recovered to 97.3%, and after photoinhibition of 31.2% at an exposure of 2 000 µmol m^{-2} s^{-1} for two hours, it reached 82.6% (Fig. 4f). In *Physcia*, the F_o/F_t ratio indicated recovery up to 100% after photoinhibition of 19% at an exposure of 1 000 µmol m^{-2} s^{-1} for one hour, and despite high light stress of 2 000 µmol m^{-2} s^{-1} for one hour, the F_o/F_t ratio remained steady, reaching up to 99.4% after photoinhibition of 12.8%. After photoinhibition of 57.2% at an exposure of 2 000 µmol m^{-2} s^{-1} for two hours, the F_o/F_t ratio recovered up to 79% (Fig. 4g). Post-hoc Tukey's tests highlighted significant recovery in *N. antarcticum* and *Physcia*, while *P. glabra* and *R. terebrata* showed greater susceptibility to photodamage.

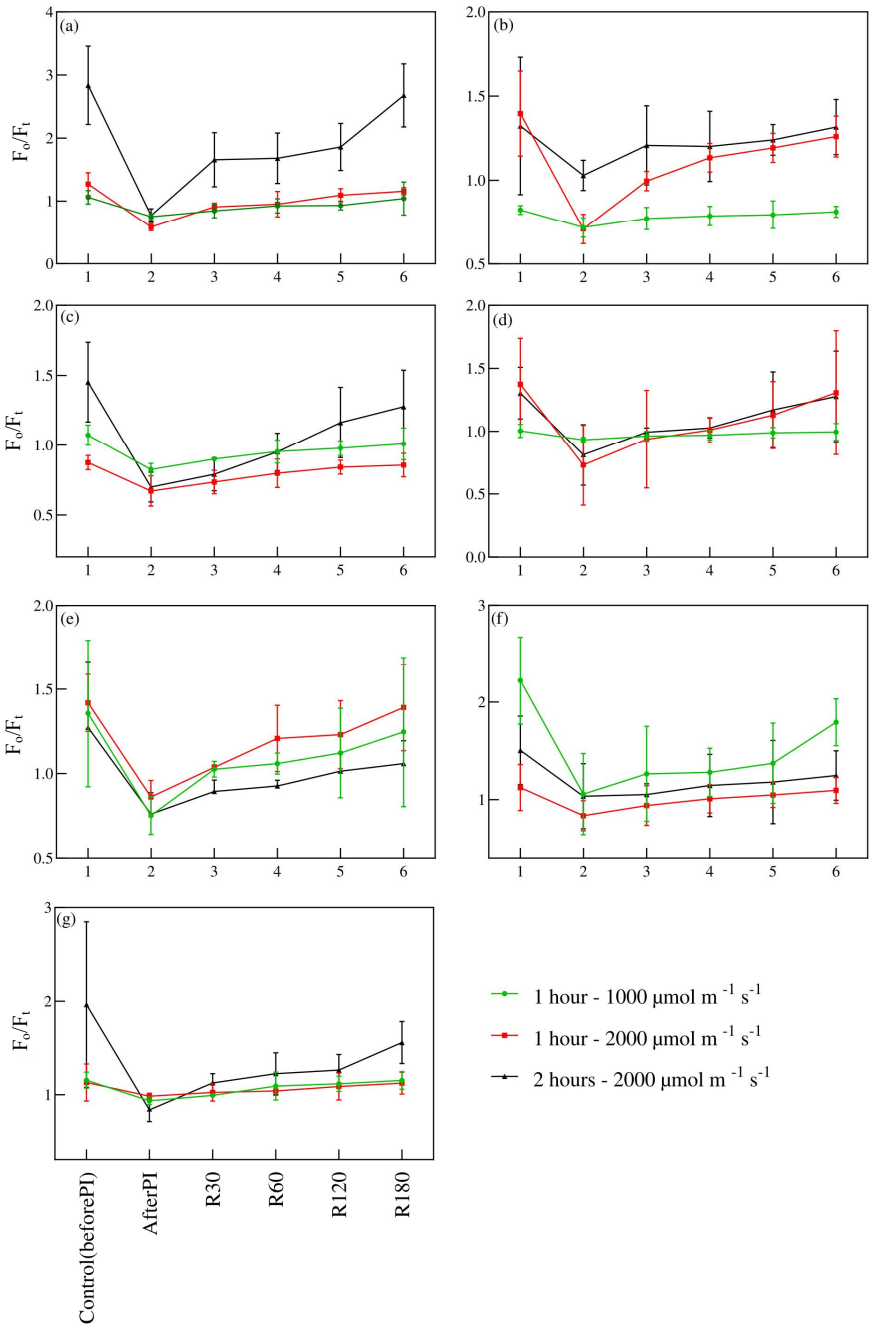

Fig. 4. Time courses of the F_o/F_t, recorded in (a) *Pseudocyphellaria glabra*, (b) *Nephroma antarcticum*, (c) *Ramalina terebrata*, (d) *Himantormia lugubris*, (e) *Cladonia* sp., (f) *Parmelia* sp. and (g) *Physcia* control (before PI), immediately after the photoinhibitory treatment (after PI), and after 30, 60, 120, and 180 min. recovery (R30, R60, R120, and R180). Data points represent the means of five replicates ± standard deviations (error bars).

Photoinhibition-induced decrease in RFD and consequent recovery

Figure 5 illustrates the recovery trends of the relative fluorescence decrease(RFD) in different lichen species following photoinhibition. ANOVA results indicated significant differences among species, light levels, and exposure times ($p < 0.05$). *P. glabra* showed increasing trends in RFD during recovery up to 96.3% after inhibition of 80.8% at an intensity of 1 000 µmol m^{-2} s^{-1} for one hour but did not completely return to control values, indicating susceptibility to prolonged exposure to intense light. After a considerable initial decrease of 89.2% at an intensity of 2 000 µmol m^{-2} s^{-1} for one hour, RFD showed complete recovery up to 100%. However, a sharp decline of 81% in RFD was observed, followed by a rise in recovery to 85% after exposure to 2 000 µmol m^{-2} s^{-1} for two hours (Fig. 5a). *N. antarcticum* showed ongoing stress with a recovery trajectory up to 90.4% after inhibition of 73% at an intensity of 1 000 µmol m^{-2} s^{-1} for one hour, indicating improvement but not fully returning to baseline. After inhibition of 79.5% at an intensity of 2 000 µmol m^{-2} s^{-1} for one hour, RFD recovered considerably to 97.8%, and after a significant initial decline of 82.2% at 2 000 µmol m^{-2} s^{-1} for two hours, it rebounded to 83.8% (Fig. 5b). *R. terebrata* recovered from photoinhibition stress, showing a varying recovery up to 94% after initial photoinhibition of 77.6% at an intensity of 1 000 µmol m^{-2} s^{-1} for one hour. After inhibition of 68.6% at an intensity of 2 000 µmol m^{-2} s^{-1} for one hour, RFD recovered to 100%, and after inhibition of 65% at 2 000 µmol m^{-2} s^{-1} for two hours, it improved to 92.8% (Fig. 5c). *H. lugubris* showed resilience to photoinhibitory conditions, with RFD rising to 96.5% after inhibition of 60.8% at an intensity of 1 000 µmol m^{-2} s^{-1} for one hour. After a significant decline of 58.4% at an intensity of 2 000 µmol m^{-2} s^{-1} for one hour, RFD gradually recovered to 98.3%. After a decline of 72.4% at an intensity of 2 000 µmol m^{-2} s^{-1} for two hours, RFD progressively rose to 91.1% (Fig. 5d). In *Cladonia* sp., the RFD showed a slight increase in recovery up to 97.3% after an initial decline of 59.7% at an intensity of 1 000 µmol m^{-2} s^{-1} for one hour. After a noticeable stress response and gradual rise, RFD recovered up to 98.3% after inhibition of 89.7% at an intensity of 2000 µmol m^{-2} s^{-1} for one hour. During the recovery phase, *Cladonia* sp. showed final recovery up to 70.8% after initial inhibition of 61.3% at an intensity of 2000 µmol m^{-2} s^{-1} for two hours (Fig. 5e). In *Parmelia* sp. the recovery phase showed a gradual increase in RFD, reaching 75% after an initial decrease of 53.1% at an intensity of 1 000 µmol m^{-2} s^{-1} for one hour, indicating ongoing stress despite signs of recovery. After a severe initial fall of 65% at an intensity of 2 000 µmol m^{-2} s^{-1} for one hour, RFD mildly rebounded to 86.3%. After an initial decline of 63.9% at an intensity of 2 000 µmol m^{-2} s^{-1} for two hours, RFD showed a modest rebound to 76.9% (Fig. 5f). In *Physcia*, RFD declined dramatically by 83.3% after exposure to 1 000 µmol m^{-2} s^{-1} for one hour but gradually improved in recovery phases, reaching up to 84.2%, indicating sluggish recovery in overall vigor. After a sharp decline of 74% at an intensity of 2 000 µmol m^{-2} s^{-1} for one hour, RFD gradually recovered to 90.2%, and after initial stress of 79.8% at 2 000 µmol m^{-2} s^{-1} for two hours, RFD recovered to only 94% (Fig. 5g). Post-hoc Tukey's tests highlighted significant recovery in *N. antarcticum* and *R. terebrata*, while *P. glabra* and *Physcia* showed greater susceptibility to photodamage.

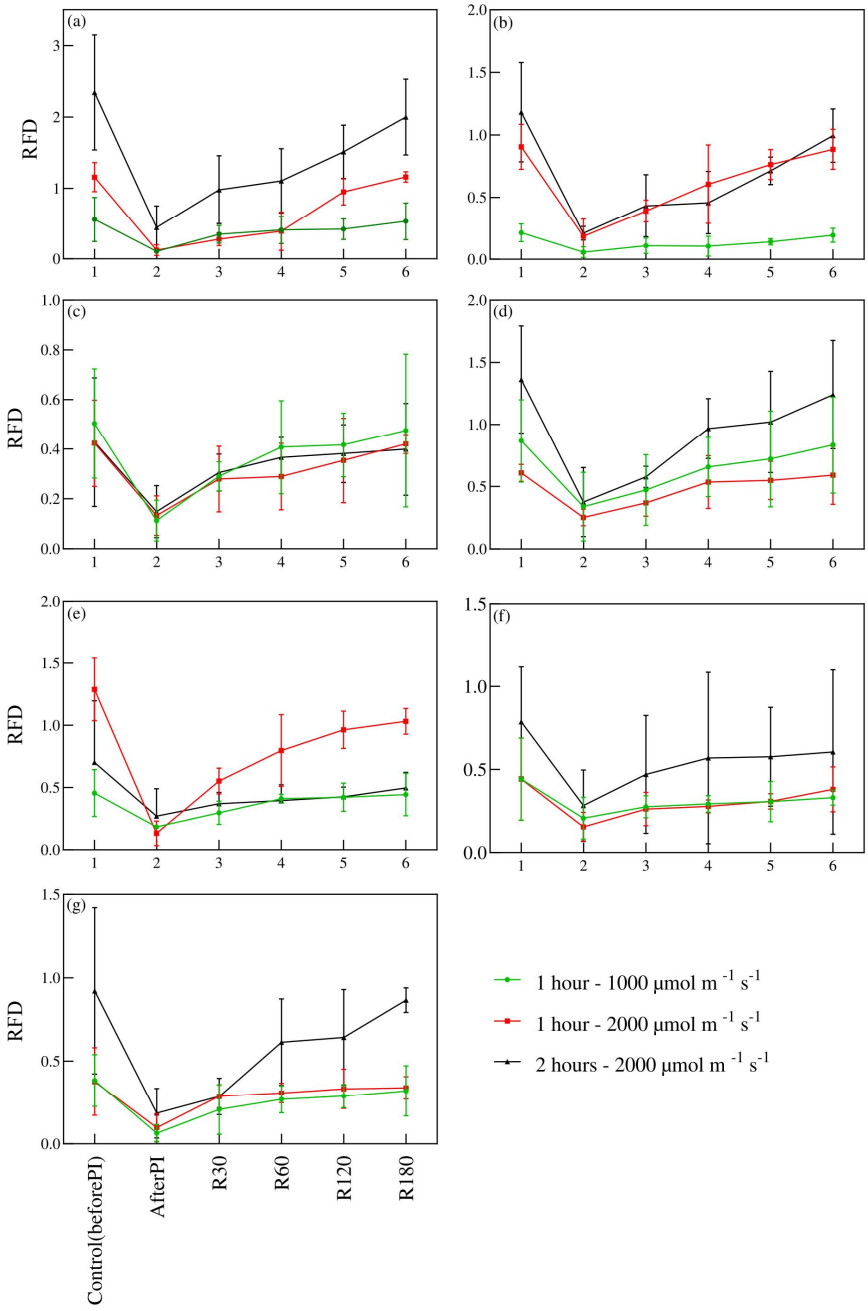

Fig. 5. Time courses of the relative fluorescence decrease (RFD), recorded in (a) *Pseudocyphellaria glabra*, (b) *Nephroma antarcticum*, (c) *Ramalina terebrata*, (d) *Himantormia lugubris*, (e) *Cladonia* sp., (f) *Parmelia* sp., and (g) *Physcia* control (before PI), immediately after the photoinhibitory treatment (after PI), and after 30, 60, 120, and 180 min. recovery (R30, R60, R120, and R180). Data points represent the means of five replicates ± standard deviations (error bars).

Dynamic non-photochemical quenching responses to photoinhibitory treatment

Figure 6 illustrates the non-photochemical quenching (NPQ) response of Antarctic and sub-Antarctic lichen species exposed to various photoinhibitory light intensities: 1 000 µmol m^{-2} s^{-1} for one hour, and 2 000 µmol m^{-2} s^{-1} for one and two hours, followed by recovery periods. ANOVA results indicated significant differences among species, light levels, and exposure times ($p < 0.01$). *P. glabra* showed a moderate increase in NPQ after exposure, indicating a stress response, followed by a gradual decrease during recovery. At a higher intensity of 2 000 µmol m^{-2} s^{-1}, a more pronounced initial increase in NPQ was observed, suggesting a stronger stress response, with a subsequent decline indicating recovery over time (Fig. 6a). *N. antarcticum* experienced a significant increase in NPQ immediately after exposure to 2 000 µmol m^{-2} s^{-1} for two hours, indicating a strong stress response. This NPQ level then gradually decreased during recovery, suggesting partial restoration of photosynthetic efficiency. At lower light intensities, NPQ levels fluctuated less and remained lower and more stable, indicating a less pronounced stress response or better resilience under those conditions (Fig. 6b). *R. terebrata* showed an intense protective response at an exposure of 1 000 µmol m^{-2} s^{-1}, with a sharp peak in NPQ immediately following photoinhibition, followed by a significant decrease as recovery began. NPQ values returned closer to baseline levels by the end of the recovery period. At a higher light intensity of 2 000 µmol m^{-2} s^{-1} for one and two hours, the peaks were less pronounced, and the overall stress response was steadier (Fig. 6c). *H. lugubris* exhibited a reactive increase in NPQ, peaking after photoinhibition and then gradually declining over the recovery periods. At lower intensities (1 000 µmol m^{-2} s^{-1} for one hour), NPQ levels remained the lowest, suggesting lesser intensity or more effective recovery mechanisms (Fig. 6d). *Cladonia* sp. showed a sharp peak in NPQ immediately after photoinhibition at both 1 000 and 2 000 µmol m^{-2} s^{-1} intensities for one hour, indicating rapid activation of protective mechanisms. NPQ values then declined notably during recovery, approaching baseline levels, indicating recovery of photosynthetic efficiency. NPQ showed the most pronounced reaction at an intensity of 2 000 µmol m^{-2} s^{-1} for two hours, with a sharp peak and a slower decline, indicating sustained stress or slower recovery (Fig. 6e). *Parmelia* sp. demonstrated a strong stress response with a sharp peak in NPQ at an intensity of 2 000 µmol m^{-2} s^{-1} for two hours, followed by a noticeable decline, although NPQ levels remained elevated relative to control, suggesting some sustained stress. At intensities of 1 000 and 2 000 µmol m^{-2} s^{-1} for one hour, NPQ showed more moderate increases, with 1 000 µmol m^{-2} s^{-1} consistently maintaining the lowest NPQ throughout the experiment (Fig. 6f). *Physcia* showed a peak in NPQ immediately after photoinhibition at an intensity of 1 000 µmol m^{-2} s^{-1} for one hour, with a steady decline during recovery, suggesting effective protective mechanisms. At an intensity of 2 000 µmol m^{-2} s^{-1} for one hour, NPQ showed a similar pattern but with a slightly higher peak, indicating more intense stress. However, at an intensity of 2 000 µmol m^{-2} s^{-1} for two hours, NPQ demonstrated the highest peak, indicating the most severe stress response, with a gradual decrease over the recovery period (Fig. 6g). Post-hoc Tukey's tests highlighted significant recovery in *R. terebrata* and *Cladonia*, while *P. glabra* and *Physcia* showed greater susceptibility to photodamage.

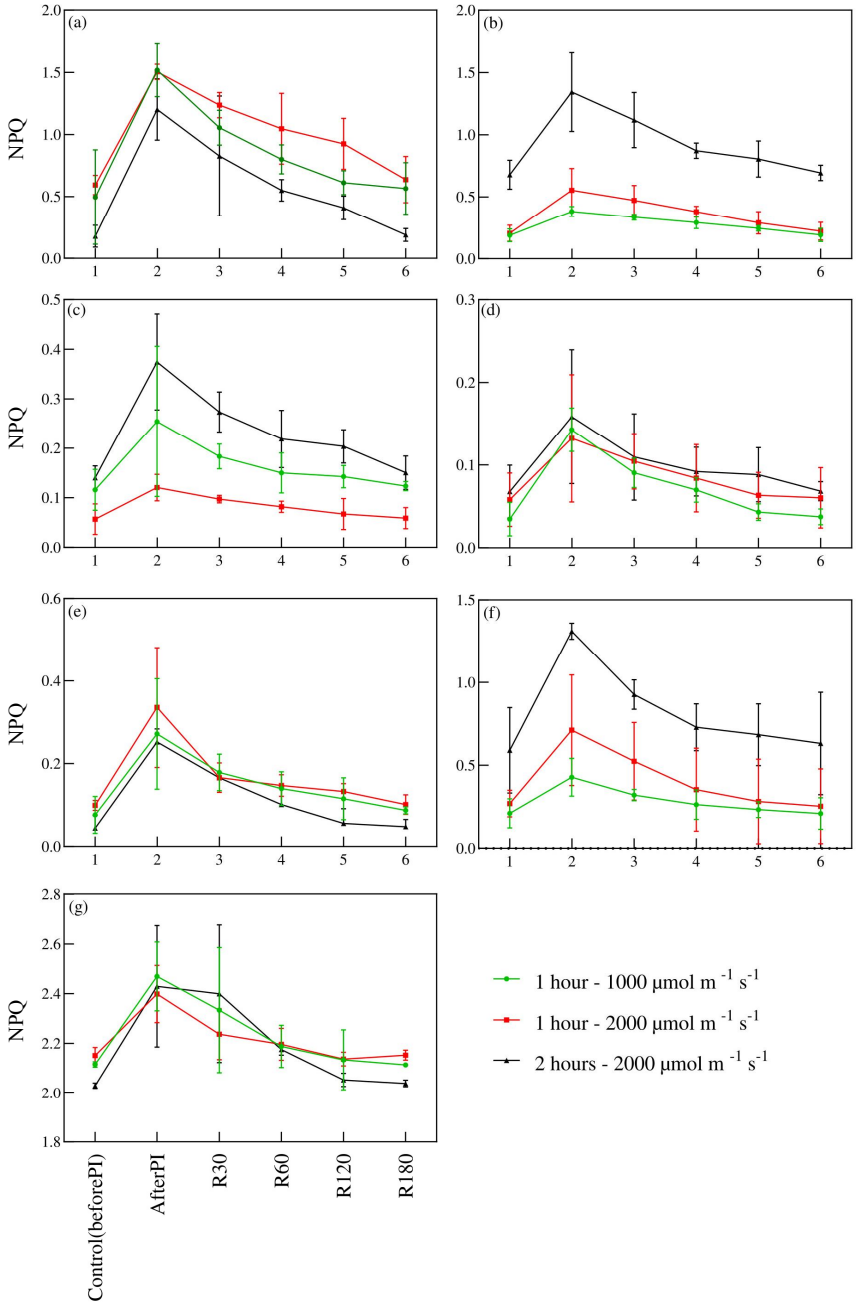

Fig. 6. Time courses of the non-photochemical quenching (NPQ), recorded in (a) *Pseudocyphellaria glabra*, (b) *Nephroma antarcticum*, (c) *Ramalina terebrata*, (d) *Himantormia lugubris*, (e) *Cladonia* sp., (f) *Parmelia* sp., and (g) *Physcia* control (before PI), immediately after the photoinhibitory treatment (after PI), and after 30, 60, 120, and 180 min. recovery (R30, R60, R120, and R180). Data points represent the means of five replicates ± standard deviations (error bars).

OJIP fluorescence profiles reflecting photoinhibition and consequent recovery

The OJIP graph illustrates varying responses to photoinhibition and recovery phases among different species (Fig. 7). General response to photoinhibitory treatment was a decrease in chlorophyll fluorescence values, forming OJIP curves found immediately after the photoinhibitory treatment (*i.e.* lowering and flattening of the curve). This phenomenon, however, was more pronounced in several species (*e.g. N. antarcticum*, *Cladonia* sp.) while it was hardly distinguishable in other ones (*e.g. H. lugubris*). *N. antarcticum* exhibited a strong initial fluorescence decline apparent immediately after photoinhibitory treatment that gradually leveled off during the recovery period, indicating effective resilience to photoinhibition. In contrast, *Cladonia* sp. experienced a significant decline during the post-inhibition phase with only partial recovery, indicating persistent damage. *P. glabra* displayed an increase in fluorescence, particularly during recovery, which suggests a strong compensatory response to stress. *Parmelia* sp. showed consistent fluorescence, indicating stable photosynthesis at the level of PS II functioning regardless of stress. *Physcia* sp., exhibited a mild improvement from the post photoinhibition state during its recovery, indicating that it possesses effective protective mechanisms against photoinhibition. OJIPs recorded in *H. lugubris*, thanks to the black colour of thallus (*see* more in Discussion) showed minimal changes throughout the phases, indicating potential vulnerability and lack of effective recovery. During photoinhibition, *R. terebrata* showed a moderate decrease in chlorophyll fluorescence that was only partially recovered, indicating some resilience and an inability to fully restore photosynthetic efficiency. These fluorescence profiles provided insights into each species' capacity to handle and recover from light-induced stress, highlighting the variability in their photoprotective and recovery mechanisms.

Temporal dynamics of photosynthetic performance index (PI_{ABS}) in lichen species after exposure to photoinhibitory treatment

The photosynthetic performance index (PI_{ABS}) for various lichen species after photoinhibitory treatment, as shown in Fig. 8, revealed diverse adaptive responses. Figure 8a illustrates a continuous increase in PI_{ABS} for *P. glabra* indicating enhanced photosynthetic efficiency during recovery. *N. antarcticum* demonstrated strong resilience, with a significant rebound in PI_{ABS} after an initial drop, indicating an effective recovery mechanism. *R. terebrata* exhibited minimal fluctuations in PI_{ABS}, reflecting stable photosynthetic activity throughout the experiment. *H. lugubris* and *Physcia* sp. displayed variable PI_{ABS} patterns but generally indicated recovery over time. *Cladonia* sp. maintained relatively steady PI_{ABS} values, suggesting consistent photosynthetic performance. In contrast, *Parmelia* sp., experienced a slight decrease in PI_{ABS}, which may suggest some difficulties in fully overcoming the photoinhibitory stress. Each species' response underscores different strategies to manage and recover from light-induced stress, highlighting the ecological versatility and resilience of lichens in adapting to harsh conditions.

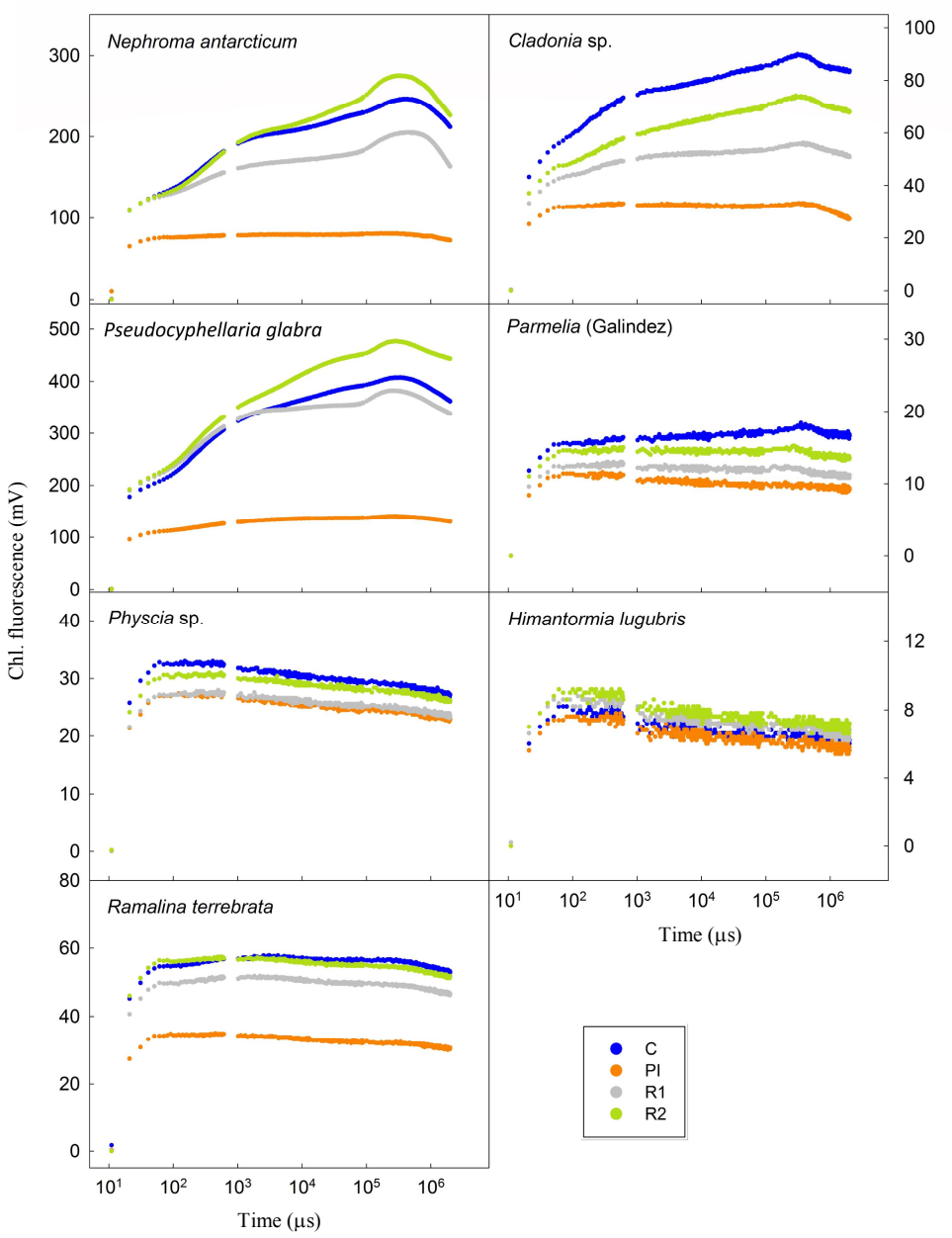

Fig. 7. Time courses of OJIP fluorescence progression, reflecting the photosynthetic efficiency of Photosystem II in various lichen species under distinct stress and recovery scenarios. Observations were made for *Nephroma antarcticum*, *Pseudocyphellaria glabra*, *Cladonia* sp., *Parmelia* sp., *Physcia* sp., *Himantormia lugubris*, and *Ramalina terebrata*. The graphs illustrate fluorescence responses from the control condition (C), immediately post-photoinhibitory treatment (2 hours PI at 2 000 µmol $m^{-2} s^{-1}$), and during two recovery intervals (R1, R2). Time is plotted on a logarithmic scale on the X-axis, while fluorescence intensity is displayed on the Y-axis. Each data point represents an average of five replicates.

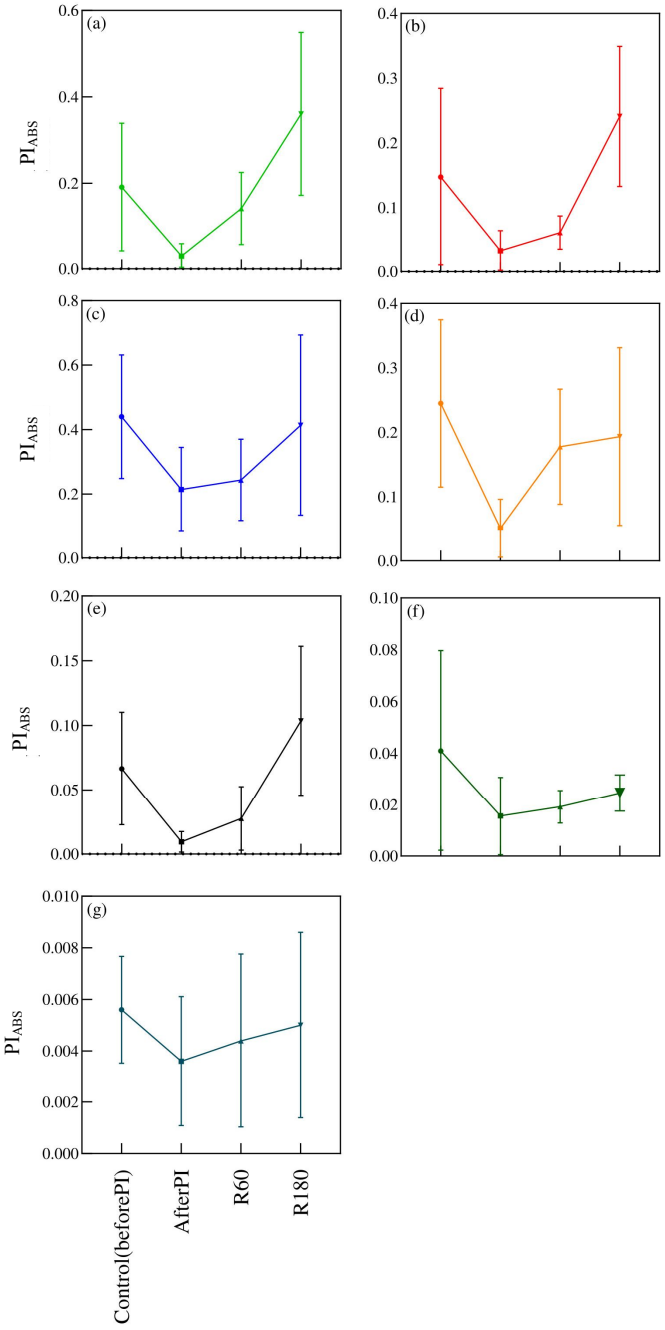

Fig. 8. Time courses of the photosynthetic performance index (PI_{ABS}), recorded in (a) *Pseudocyphellaria glabra*, (b) *Nephroma antarcticum*, (c) *Ramalina terebrata*, (d) *Himantormia lugubris*, (e) *Cladonia* sp., (f) *Parmelia* sp., and (g) *Physcia* control (before PI), immediately after the photoinhibitory treatment (after PI), and after 60 and 180 min. recovery (R60 and R180). Data points represent the means of five replicates ± standard deviations (error bars).

Electron transport rate dynamics in lichen species after photoinhibitory treatment and during recovery phases

Fig. 9a illustrates that after photoinhibition, *P. glabra* experienced a noticeable decline in ETR with a slight recovery by R180, indicating a temporary impact of light stress on photosynthetic electron transport, with some potential for recovery. Similarly, *N. antarcticum* exhibited an initial drop in ETR post-treatment, followed by a significant rise during recovery (Fig. 9b). This indicated not only resilience but also an enhancement in photosynthetic capacity under recovery conditions. Figure 9c illustrates that *R. terebrata* experienced a rapid decrease in ETR immediately after treatment and a partial recovery by R180, indicating susceptibility to photoinhibition and a gradual recovery process. *H. lugubris* displayed a sharp decrease in ETR after treatment, followed by a dramatic rebound at R60, before declining again (Fig. 9d). *Cladonia* sp. maintained a relatively steady ETR with minor fluctuations, reflecting stable photosynthetic activity (Fig. 9e). *Parmelia* sp. exhibited a significant increase in ETR at R60, suggesting a strong but possibly temporary rebound in photosynthetic efficiency (Fig. 9f). *Physcia*, on the other hand, showed a slight but steady decrease in ETR from control through recovery, indicating a mild but continuous effect of photoinhibition on electron transport efficiency (Fig. 9g). These distinct patterns highlight the varied strategies lichens employ to cope with and adapt to photoinhibitory conditions.

Dynamics of dissipation in lichen species after photoinhibitory treatment and during recovery phases

Fig. 10 shows the dissipation index (DI_o/RC) for seven lichen species at different stages: control, immediately after photoinhibitory treatment, and during recovery phases at 60 and 180 minutes. *P. glabra* exhibited a significant increase in DI_o/RC after treatment, indicating a strong dissipative response, which then sharply decreased by R60 (Fig. 10a). *N. antarcticum* displayed a similar peak post-treatment, followed by a significant reduction, indicating rapid recovery (*see* Fig. 10b). *R. terebrata* maintained relatively stable DI_o/RC levels, indicating consistent energy dissipation across all phases (Fig. 10c). (Fig. 10c). *H. lugubris* showed varying dissipation rates, peaking at R60 (Fig. 10d). *Cladonia* sp. demonstrated a peak at control, followed by a decrease post-treatment and a slight recovery by R180 (Fig. 10e). *Parmelia* sp. exhibited a significant increase in dissipation at R60, indicating a delayed response to stress (*see* Fig. 10f). Lastly, *Physcia* maintained steady DI_o/RC levels, indicating minimal changes in energy dissipation across the measured periods (Fig. 10g). These patterns highlight the diverse strategies of lichens in managing energy not utilized in photochemistry under stress and recovery conditions.

Correlation analysis between F_V/F_M and PI_{ABS}

The correlation plot showed a positive relationship between the maximal quantum yield of PSII (F_V/F_M) and the Performance Index on an absorption basis (PI_{ABS}) among various lichen species (Fig. 11).

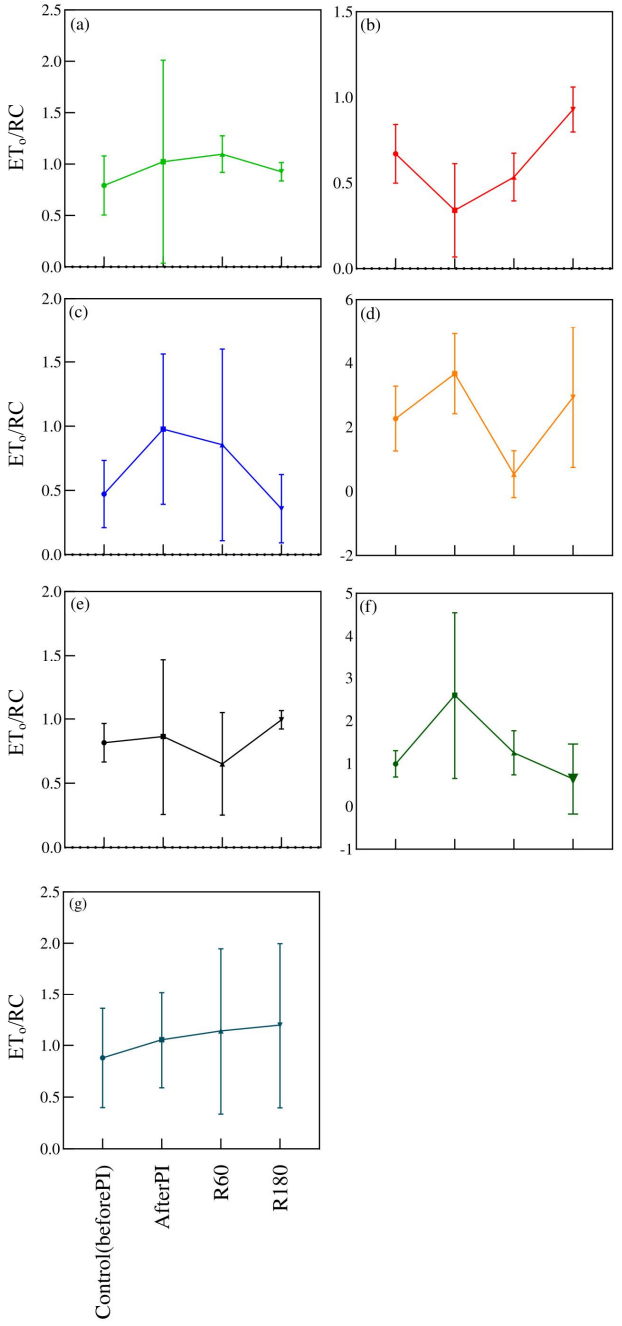

Fig. 9. Time courses of the electron transport (ET_o/RC), recorded in (a) *Pseudocyphellaria glabra*, (b) *Nephroma antarcticum*, (c) *Ramalina terebrata*, (d) *Himantormia lugubris*, (e) *Cladonia* sp., (f) *Parmelia* sp., and (g) *Physcia* control (before PI), immediately after the photoinhibitory treatment (after PI), and after 60 and 180 min. recovery (R60 and R180). Data points represent the means of five replicates ± standard deviations (error bars).

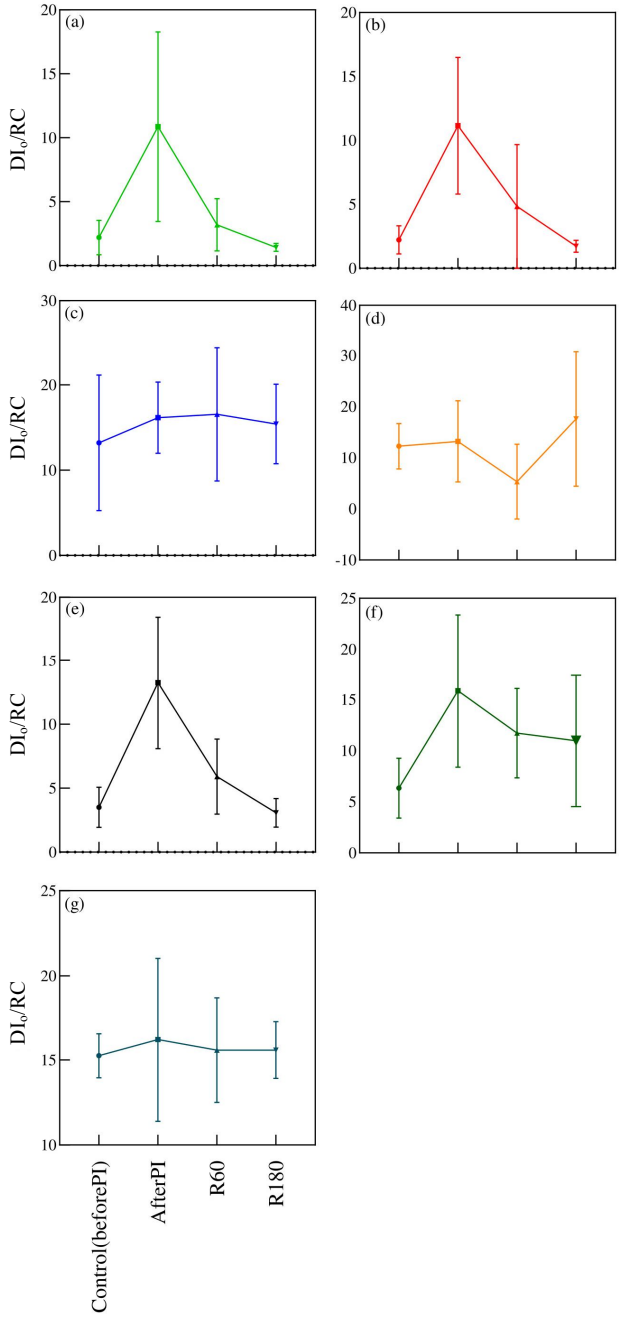

Fig. 10. Time courses of the dissipation (DI_o/RC), recorded in (a) *Pseudocyphellaria glabra*, (b) *Nephroma antarcticum*, (c) *Ramalina terebrata*, (d) *Himantormia lugubris*, (e) *Cladonia* sp., (f) *Parmelia* sp., and (g) *Physcia* control (before PI), immediately after the photoinhibitory treatment (after PI), and after 60 and 180 min. recovery (R60 and R180). Data points represent the means of five replicates ± standard deviations (error bars).

Data under control conditions generally appear in the upper right quadrant, displaying high values for both F_V/F_M and PI_{ABS}, which indicates optimal photosynthetic efficiency and minimal stress. Following exposure to photoinhibitory stress, a clear migration of data points toward lower values for both metrics was observed, aligning with expectations that stress diminishes photochemical yield and overall performance. During the recovery phase, many species demonstrated a trend towards recovery, evidenced by their movement back towards higher values, although not consistently returning to baseline levels. This behaviour across different conditions confirms the correlation between higher photochemical yields and better stress management capabilities in lichens, supporting the scientific understanding of their adaptive responses to environmental stresses.

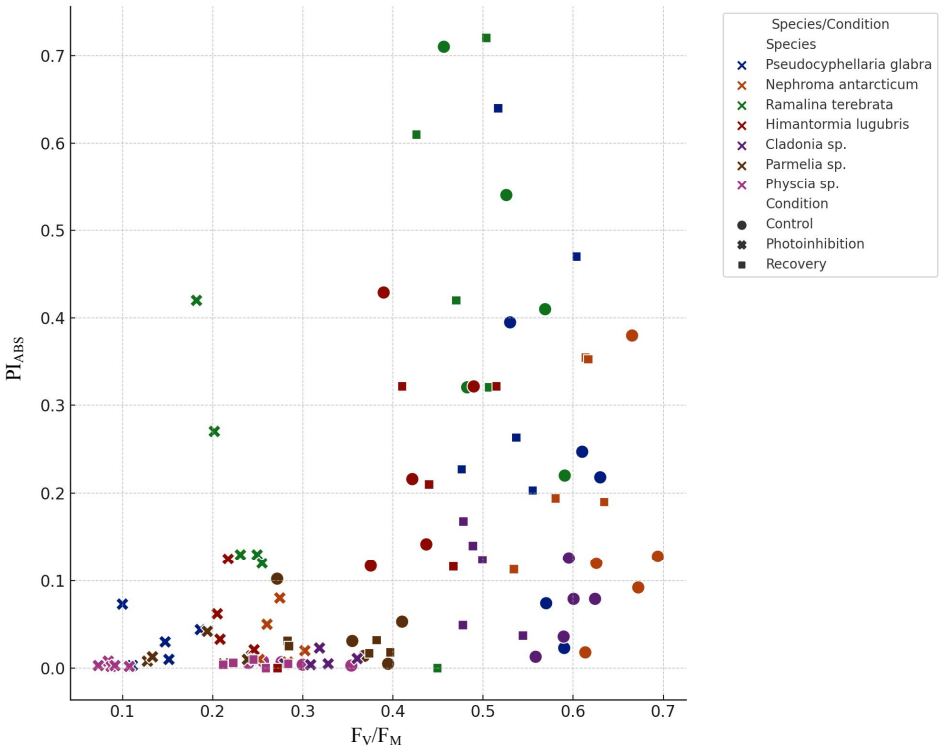

Fig. 11. Correlation between F_V/F_M and PI_{ABS} across lichen species and conditions.

Discussion

This research comprehensively examined the impact of photoinhibition and the ensuing recovery processes under varying light exposure in lichens located in the Antarctic and Subantarctic regions. Time courses of F_V/F_M and Φ_{PSII} recorded during photoinhibitory treatment showed similar shapes to those recorded for a variety of photoinhibited lichen species (Barták et al. 2004, Balarinová et al. 2014), *i.e.*, a photoinhibition-induced decline with consequent recovery with well-distinguished

fast- and slow-phase. The recovery dynamics within the first 30 minutes of photoinhibitory treatment show significant decrease across the studied lichen species. There is an average reduction of 32% from the initial photosynthetic capacity for F_V/F_M and 34% for Φ_{PSII}, indicating significant photoprotection engagement but not reaching baseline levels. At the end of the recovery period, the 30-minute values show further decreases of 27% for F_V/F_M and 29% for Φ_{PSII} relative to the final recovery states, highlighting ongoing recovery processes. Such a fast and effective fast phase of recovery indicates the sufficient capacity of photoprotective mechanisms to cope with photoinhibition which is reported in lichens from sunny habitats (*e.g.* Singh et al. 2013). In lichens, mechanisms comprise quenching of excitation energy via high light-induced violaxanthin to zeaxanthin conversion (Demmig-Adams et al. 1990), the state 1-2 transition (Wendler *e.g.* Veerman et al. 2007), and structural changes in the arrangement of PS II supercomplex (Kosugi et al. 2018). These findings imply that lichens quickly activate photoprotective responses to efficiently reduce initial photodamage, demonstrating their ecological adaptations and inherent resilience to high light stress.

The time courses showed species-specific and dose-dependent differences, however, in general, they were comparable to the data presented for Antarctic lichen species (Barták et al. 2004, 2023). Our results indicate almost full recovery of F_V/F_M and Φ_{PSII} after 3 hours from the termination of the photoinhibitory treatment which indicates a high capacity of the experimental species to cope with short-term strong photoinhibition. Among the investigated species, *R. terebrata* showed the least resistance to photoinhibition compared to *P. glabra*, *N. antarcticum*, *H. lugubris*, *Cladonia* sp., *Parmelia* sp., and *Physcia* genera. *R. terebrata* showed significant initial photodamage as reflected by a sharp decrease in the F_V/F_M ratio following exposure to intense light. Although there was some recovery noted, the F_V/F_M ratios remained below initial levels, indicating ongoing stress. During the recovery phase, the quantum yield parameter Φ_{PSII} showed signs of improvement but did not return to baseline values, highlighting a compromised restoration of photosynthetic efficiency. Furthermore, the partial recovery observed in the F_o/F_t ratio underscores the species' difficulty in fully returning to control conditions, with the relative fluorescence decrease (RFD) also indicating similar trends of incomplete recovery. Additionally, NPQ peaks early and declines sharply, indicating a strong but transient photoprotective response (Fig. 2-6). *N. antarcticum* and *H. lugubris* both suffered significant photodamage. Although they somewhat recovered, they did not return to their initial states. *Physcia* experienced initial damage but recovered better than the previous two, indicating a more robust adaptation to high-light stress. *P. glabra* showed strong resilience with a robust recovery, indicating effective photoprotection. *Parmelia* sp., and *Cladonia* sp., demonstrated varying levels of resistance and recovery capacity, with *Parmelia* sp., showing substantial recovery, and *Cladonia* sp., effectively mitigating initial damage and almost completely restoring its photosynthetic capacity, displaying superior adaptive strategies. These species' varied responses showcase their diverse physiological and ecological adaptations to cope with intense light environment (Fig. 2-6).

Fast recovery F_V/F_M and Φ_{PSII} might be associated with a high capacity of lichen photosynthetic apparatus to cope with high light stress thanks to activation of protective mechanisms associated with non-photochemical quenching (NPQ), which generally increases in high light-treated lichens in hydrated state (Vráblíková et al. 2005). Increased NPQ is typically recorded in lichens after tens of seconds of high-light treatment. Apart from such physiological short-term responses, some consti-

tutive ones protect photobiont cells due to the high absorption of light in the upper cortex. Such a mechanism is allowed by the presence of melanins that are synthesized by the fungal partner and absorb incident light both in the UV and PAR parts of the spectrum. Therefore, melanized lichens are rather resistant to photoinhibition (Mafole et al. 2019). In Antarctic and Subantarctic lichens, several other substances synthesized by a fungal partner play a role in photoprotection in lichens from sunny microhabitats. They are typically studied by acetone rinsing method (*see* e.g. Solhaug and Gauslaa 1996, Carniel et al. 2017) and consequent absorption spectra of the extract (for Umbilicariaceae *see* e.g. Martic et al. 2016).

The shape of slow Kautsky kinetis (KK) of chlorophyll fluorescence recorded during an exposition to actinic light is affected by photoinhibitory treatment and activation of photoinhibitory treatment-induced quenching mechanisms. This leads to an overall decrease in chlorophyll fluorescence signals distinguished on the KK, *i.e.* O, P, M, S, T. For photoprotection, a decrease in background chlorophyll fluorescence (F_o) is of great importance since it relates to the chlorophyll fluorescence signal emitted from light-harvesting complexes (LHCs). Photoinhibition-induced decrease in F_o (*see* Fig. 2-6) is associated with protective mechanisms consisting of the light-induced detachment of LHCs, their aggregation and effective quenching of absorbed light energy. Moreover, state 1-2 transition plays a role in some photoinhibited lichens providing a pathway for LHC deenergitization thanks to delivery of absorbed light energy to PS I. Therefore, F_o decrease is a short-term response of lichen photosynthetic apparatus to photoinhibitory treatment. It is well documented, that F_o decreases immediately after a lichen sample is exposed to experimental light of about 2 000 μmol m^{-2} s^{-1}. Photoinhibition-induced negative changes to PS II functioning are well-documented in the decrease in RFD apparent in all experimental species when measured immediately after the termination of photoinhibitory treatment. Since RFD is considered a general description of the vitality of photosynthetic apparatus, it might be concluded that all experimental lichen species showed a reversible response and achieved almost 100% recovery indicating that they might be ranked as photoinhibition resistant. OJIPS methodologies offer insight into the photosynthetic resilience, recovery patterns, and robustness of lichen species. *P. glabra* demonstrates significant resilience. Their photosynthetic performance index (PI_{ABS}) shows a continuous increase after photoinhibitory treatment, suggesting an efficient recovery mechanism due to an advanced antioxidative defense system (Fig. 8). *N. antarcticum* also demonstrates strong recovery dynamics, with significant rebounds in PI_{ABS} and electron transport rate (ETR), indicating its robust adaptive mechanisms to quickly restore photosynthetic efficiency post-stress (Fig. 8, 9). Conversely, *Parmelia* sp. experiences a slight decrease in PI_{ABS} and struggles to fully overcome photoinhibitory stress (Fig. 8). This vulnerability could reflect a less efficient photoprotective response, potentially limiting its distribution and abundance in harsh environments. *R. terebrata* maintains minimal fluctuations in PI_{ABS} throughout the experimental period (Fig. 8), reflecting stable photosynthetic activity that may be attributed to its structural and physiological traits buffering against extreme conditions. *H. lugubris* and *Physcia*, although displaying variable patterns in PI_{ABS} and ETR, generally indicate recovery over time (Fig. 8, 9). This may be attributed to their flexible metabolic adjustments during stress recovery phases. Lastly, *Cladonia* maintains relatively stable PI_{ABS} values and experiences minor ETR fluctuations, indicating consistent photosynthetic performance and a potential evolutionary advantage in persisting under varying environmental stresses (Fig. 8, 9).

Morphological traits play a crucial role in determining the susceptibility and resilience of lichens to photoinhibition. The structural characteristics, such as thallus thickness and the arrangement of photobiont layers, can significantly impact how light is absorbed and dissipated within the thallus. These traits may help explain why some species exhibit better recovery rates than others. For instance, thicker thalli may provide more substantial protection against intense light, aiding in the dissipation of excess energy and reducing the incidence of photoinhibition (Armstrong 2017). These interspecific differences show the resilience and ecological versatility of lichens, demonstrating the various adaptive strategies that allow these organisms to survive in extreme conditions. Our study not only expands the understanding of lichen photobiology but also contributes to predicting the responses of polar biota to increasing photodynamic pressures.

References

AKINYEMI, O. O., ČEPL, J., KESKI-SAARI, S., TOMÁŠKOVÁ, I., STEJSKAL, J., KONTUNEN-SOPPELA, S. and KEINÄNEN, M. (2023): Derivative-based time-adjusted analysis of diurnal and within-tree variation in the OJIP fluorescence transient of silver birch. *Photosynthesis Research*, 157(2): 133-146.

ARMSTRONG, R. A. (2017): Adaptation of lichens to extreme conditions. *In*: V. Shukla, S. Kumar, N. Kumar (eds): Plant Adaptation Strategies in Changing Environment. Springer, Singapore, pp. 1–27.

ARMSTRONG, R. A. (2021): The potential of pioneer lichens in terraforming Mars. *Terraforming Mars*, 533-553.

AUCIQUE-PEREZ, C. E., RAMOS, A. E. R. (2024): Chlorophyll *a* fluorescence: A method of biotic stress detection. *IntechOpen*. doi: 10.5772/intechopen.1004830

BALARINOVÁ, K., BARTÁK, M., HAZDROVÁ, J., HÁJEK, J. and JÍLKOVÁ, J. (2014): Changes in photosynthesis, pigment composition and glutathione contents in two Antarctic lichens during a light stress and recovery. *Photosynthetica*, 52: 538-547.

BARTÁK, M., HÁJEK, J., HALICI, M. G., BEDNAŘÍKOVÁ, M., CASANOVA-KATNY, A., VÁCZI, P., PUHOVKIN, A., MISHRA, K. B. and GIORDANO, D. (2023): Resistance of primary photosynthesis to photoinhibition in Antarctic lichen *Xanthoria elegans*: Photoprotective mechanisms activated during a short period of high light stress. *Plants*, 12(12): 2259. doi: 10.3390/plants12122259

BARTÁK, M., HÁJEK, J., OREKHOVA, A., VILLAGRA, J., MARÍN, C., PALFNER, G. and CASANOVA-KATNY, A. (2021): Inhibition of primary photosynthesis in desiccating antarctic lichens differing in their photobionts, thallus morphology, and spectral properties. *Microorganisms*, 9(4): 818.

BARTÁK, M., HÁJEK, J., VRÁBLÍKOVÁ, H. and DUBOVÁ, J. (2004): High-light stress and photoprotection in *Umbilicaria antarctica* monitored by chlorophyll fluorescence imaging and changes in zeaxanthin and glutathione. *Plant Biology*, 6(03): 333-341.

CARNIEL, F. C., PELLEGRINI, E., BOVE, F., CROSERA, M., ADAMI, G., CRISTINA, NALI, C., LORENZINI, G. and TRETIACH, M. (2017): Acetone washing for the removal of lichen substances affects membrane permeability. *The Lichenologist*, 49(4): 387-395. doi: 10.1017/S0024282917000263

CARR, E. C., HARRIS, S. D., HERR, J. R. and RIEKHOF, W. R. (2021): Lichens and biofilms: Common collective growth imparts similar developmental strategies. *Algal Research*, 54: 102217.

COLESIE, C., WALSHAW, C. V., SANCHO, L. G., DAVEY, M. P. and GRAY, A. (2023): Antarctica's vegetation in a changing climate. *Wiley Interdisciplinary Reviews: Climate Change*, 14(1): e810.

DEMMIG-ADAMS, B., MÁGUAS, C., ADAMS, W. W., MEYER, A., KILIAN, E. and LANGE, O. L. (1990): Effect of high light on the efficiency of photochemical energyconversion in a variety of lichen species with green and bluegreen phycobionts. *Planta*, 180: 400-409. doi: 10.1007/BF00198792

KHAN, N., ESSEMINE, J., HAMDANI, S., QU, M., LYU, M. J. A., PERVEEN, S., STIRBET, A., GOVINDJEE, G. and ZHU, X. G. (2021): Natural variation in the fast phase of chlorophyll a fluorescence induction curve (OJIP) in a global rice minicore panel. *Photosynthesis Research*, 150: 137-158. doi: 10.1007/s11120-020-00794-z

KOHZUMA, K., SONOIKE, K. and HIKOSAKA, K. (2021): Imaging, screening and remote sensing of photosynthetic activity and stress responses. *Journal of Plant Research*, 134(4): 649-651.

KOSUGI, M., MARUO, F., INOUE, T., KUROSAWA, N., KAWAMATA, A., KOIKE, H., KAMEI, Y., KUDOH, S. and IMURA, S. (2018): A comparative study of wavelength-dependent photoinactivation in photosystem II of drought-tolerant photosynthetic organisms in Antarctica and the potential risks of photoinhibition in the habitat. *Annals of Botany*, 122(7): 1263-1278. doi: 10.1093/aob/mcy139

MAFOLE, T. C., CHIANG, C., SOLHAUG, K. A. and BECKETT, R. P. (2017): Melanisation in the old forest lichen Lobaria pulmonaria reduces the efficiency of photosynthesis. *Fungal Ecology*, 29: 103-110.

MAFOLE, T. C., SOLHAUG, K. A., MINIBAYEVA, F. V. and BECKETT, R. P. (2019): Tolerance to photoinhibition within lichen species is higher in melanised thalli. *Photosynthetica*, 57(1): 96-102. doi: 10.32615/ps.2019.008

MARTIC, L. (2016): Lichen secondary metabolites in *Umbilicaria antarctica* evaluated by acetone rinsing. *Czech Polar Reports*, 6(2): 186-190.

NDHLOVU, N. T., MINIBAYEVA, F., SMITH, F. R. and BECKETT, R. P. (2023): Lichen substances are more important for photoprotection in sun than shade collections of lichens from the same species. *The Bryologist*, 126(2): 180-190.

OREKHOVA, A., BARTÁK, M., CASANOVA-KATNY, A. and HÁJEK, J. (2021): Resistance of Antarctic moss *Sanionia uncinata* to photoinhibition: Chlorophyll fluorescence analysis of samples from the western and eastern coasts of the Antarctic Peninsula. *Plant Biology*, 23(4): 653-663.

PERERA-CASTRO, A. V., FLEXAS, J., GONZÁLEZ-RODRÍGUEZ, Á. M. and FERNÁNDEZ-MARÍN, B. (2021): Photosynthesis on the edge: Photoinhibition, desiccation and freezing tolerance of Antarctic bryophytes. *Photosynthesis Research*, 149(1): 135-153.

POSPÍŠIL, P. (2016): Production of reactive oxygen species by photosystem II as a response to light and temperature stress. *Frontiers in Plant Science*, 7: 232551.

SHI, Q., WANG, X. Q., ZENG, Z. L. and HUANG, W. (2022): Photoinhibition of photosystem I induced by different intensities of fluctuating light is determined by the kinetics of ΔpH formation rather than linear electron flow. *Antioxidants*, 11(12): 2325.

SINGH, R., RANJAN, S., NAYAKA, S., PATHRE, U. V. and SHIRKE, P. A. (2013): Functional characteristics of a fruticose type of lichen, *Stereocaulon foliolosum* Nyl., in response to light and water stress. *Acta Physiologiae Plantarum*, 35: 1605-1615.

SOLHAUG, K. A., GAUSLAA, Y. (1996): Parietin, a photoprotective secondary product of the lichen *Xanthoria parietina*. *Oecologia*, 108: 412-418.

VEERMAN, J., VASIL'EV, S., PATON, G.D., RAMANAUSKAS, J. and BRUCE, D. (2007): Photoprotection in the lichen *Parmelia sulcata*: The origins of desiccation-induced fluorescence quenching. *Plant Physiology*, 145: 997-1005.

VRÁBLÍKOVÁ, H., BARTÁK, M. and WONISCH, A. (2005): Changes in glutathione and xanthophyll cycle pigments in the high light-stressed lichens *Umbilicaria antarctica* and *Lasallia pustulata*. *Journal of Photochemistry and Photobiology B: Biology*, 79(1): 35-41.

WIENERS, P. C., MUDIMU, O. and BILGER, W. (2018): Survey of the occurrence of desiccation-induced quenching of basal fluorescence in 28 species of green microalgae. *Planta*, 248: 601-612.

ZABRET, J., NOWACZYK, M. M. (2021): OJIP chlorophyll fluorescence induction profiles and plastoquinone binding affinity of the Photosystem II assembly intermediate PSII-I from *Thermosynechococcus elongatus*. *BioRxiv*, 2021-06.

ZAVAFER, A., MANCILLA, C. (2021): Concepts of photochemical damage of Photosystem II and the role of excessive excitation. *Journal of Photochemistry and Photobiology C: Photochemistry Reviews*, 47: 100421.